DYNAMICAL ANALYSIS OF A NEW 3D CHAOTIC SYSTEM WITH COEXISTING ATTRACTORS*

Qiang Lai†, Shi-Ming Chen

School of Electrical and Electronic Engineering
East China Jiaotong University, Nanchang, 330013, China

(Received April 20, 2015; revised version received May 11, 2015)

In this paper, a new 3D chaotic system with five nonlinearities is introduced. The basic behaviors of the system are investigated. The dynamic evolution of the system is analyzed by bifurcation diagram, Lyapunov exponents, phase diagram. It is shown that the system generates chaos via Hopf bifurcation and period-doubling bifurcation with the parameters change. The coexisting attractors including point, periodic, chaotic attractors is presented. It is found that the system is abound in coexisting double homologous attractors with respect to different initial values.

DOI:10.5506/APhysPolB.46.1967
PACS numbers: 05.45.–a, 05.45.Ac, 05.45.Pq

1. Introduction

Chaos is an important nonlinear phenomena which is characterized by the initial value sensitivity. Due to its outstanding contributions in complexity science, chaos is widely regarded as the third great revolution of the 20th century occurred in physics. Since Lorenz found the first chaotic attractor for atmospheric convection [1], chaos has remained to be an academic interest to many scientists.

As the broad application prospects of chaos in engineering, the chaos generation or chaotification has been an important research topic for years. Numerous chaotic systems were constantly presented based on continuous autonomous differential equations with quadratic nonlinearities, such as Rössler system, Rucklidge system, Genesio system, Sprott system, Chen system, Lü system, no-equilibria chaotic systems, hyperchaos systems, *etc.* [2–13]. With further research, scholars discovered that some simple chaotic

* This work is supported by the National Natural Science Foundation of China under Grant 61364017.

† Corresponding author: `laiqiang87@126.com`

systems can perform coexisting attractors for different initial conditions. Leipnik and Newton earlier introduced a chaotic system with coexisting two strange attractors in separate regions of phase space [14]. In 2004, Liu *et al.* found a Lorenz-type chaotic system which generates not only four-scroll chaotic attractors but also coexisting chaotic attractors [15]. In 2010, Dadras *et al.* introduced a smooth autonomous system with coexisting symmetric chaotic attractors [16]. In 2013, Sprott *et al.* analyzed a six-term chaotic system with only one stable equilibrium with a coexistence of point, periodic and chaotic attractors [17]. Li and Sprott presented a 3D differential system with four quadratic nonlinearities, which displays five coexisting attractors with one limit cycle, two stable points and two strange attractors at some special parameters [18]. Recently, the systems with coexisting attractors have been of increasing concern in academic field for its potential engineering applications [19–21]. In many nonlinear systems, coexisting attractors with independent domains of attraction are often unavoidable. Investigation of the coexisting attractors and its internal mechanism is of significant importance for revealing the dynamic evolution of the system.

Although many chaotic systems have been established, but only in a handful of chaotic systems multiple independent attractors coexist. The chaotic systems with coexisting attractors have many key issues that need further study. Motivated by these views, we propose a new 3D dissipative chaotic system with coexisting attractors. The system has eight terms and five quadratic nonlinearities. Some basic properties of the system are analyzed. The dynamic evolution of the system is presented by bifurcation diagram, Lyapunov exponents, phase diagram. Importantly, the coexisting attractors include point, periodic, chaotic attractors. It is found that the system is abound in coexisting double homologous attractors corresponding to different initial conditions.

2. A new 3D chaotic system

A new chaotic system proposed in this letter is described as a set of three first-order, autonomous, ordinary differential equations as follows

$$\begin{cases} \dot{x} = ax - yz\,, \\ \dot{y} = -by + xz\,, \\ \dot{z} = -cz + (x+y)^2\,, \end{cases} \tag{1}$$

where x, y, z are state variables, $a > 0, b > 0, c > 0$ are all real parameters. From the composition of the equations, system (1) has eight terms and five quadratic nonlinearities. It is not identical with the existing chaotic system from the homeomorphic topological theory [22, 23]. For two vector fields $f(x), g(x) \in R^n$, satisfying dynamical systems $\dot{x} = f(x)$ and $\dot{y} = f(y)$

with $x, y \in R^n$, if there exists a diffeomorphism h on R^n such that $f(x) = M^{-1}(x)g(h(x))$, where $M(x)$ is the Jacobian of h at the point x, then the two dynamical systems are said to be smoothly equivalent. Suppose that $\dot{x} = f(x)$ and $\dot{y} = f(y)$ are smoothly equivalent, then the Jacobians at their equilibria x_0 and $y_0 = h(x_0)$ have the same characteristic equations and eigenvalues. It is obvious that two dynamical systems are nonequivalent smoothly if they have different number of equilibria. Based on these points, it can be concluded that system (1) is nonequivalent smoothly to the Lorenz system, Chen system, *etc.*

As the parameters vary, system (1) performs complex dynamical behaviors. Of particular importance is that multiple coexisting attractors with respect to different initial conditions is abound in system (1). The chaotic attractor of system (1) is revealed by selecting parameters $a = 6, b = -12, c = -5$ and initial value $x_0 = (1, 1, 1)$ as shown in Fig. 1. The chaotic characteristic of the attractor is determined by its largest Lyapunov exponent $\mathrm{LE}_1 = 0.9952 > 0$ and Poincaré map on the crossing section $z = 20$.

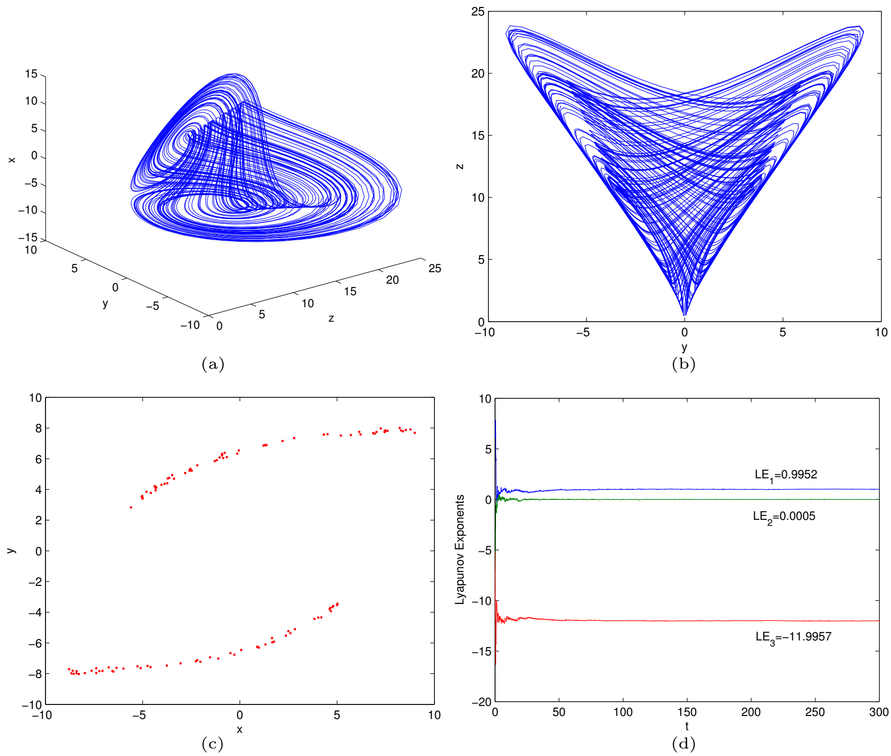

Fig. 1. (Color on-line) The chaotic attractor of system (1): (a) x–y–z; (b) y–z; (c) Poincaré section; (d) Lyapunov exponents.

3. Analysis of the equilibria

System (1) has three equilibria by solving the equations $\dot{x} = \dot{y} = \dot{z} = 0$, which are given as

$$
\begin{aligned}
&O(0,0,0)\,,\\
&O_1\left(\frac{a^{1/4}b^{3/4}c^{1/2}}{a^{1/2}+b^{1/2}}, \frac{a^{3/4}b^{1/4}c^{1/2}}{a^{1/2}+b^{1/2}}, a^{1/2}b^{1/2}\right)\,,\\
&O_2\left(-\frac{a^{1/4}b^{3/4}c^{1/2}}{a^{1/2}+b^{1/2}}, -\frac{a^{3/4}b^{1/4}c^{1/2}}{a^{1/2}+b^{1/2}}, a^{1/2}b^{1/2}\right)\,.
\end{aligned}
$$

It is easy to verify that O is an unstable point since it has a positive real eigenvalue $\lambda_1 = a > 0$ of the corresponding characteristic equation.

The Jacobian matrix of system (1) at O_i $(i = 1, 2)$ is

$$
J = \begin{pmatrix} a & -z & -y \\ z & -b & x \\ 2(x+y) & 2(x+y) & -c \end{pmatrix}.
$$

By using $|\lambda I - J| = 0$, the corresponding characteristic equation of J is obtained as

$$
\lambda^3 + (b+c-a)\lambda^2 + \frac{c(a+b)\left(b^{1/2}-a^{1/2}\right)}{a^{1/2}+b^{1/2}}\lambda + 4abc = 0\,. \tag{2}
$$

According to the Routh–Hurwitz criterion, O_i is a stable point as long as the following conditions are satisfied

$$
\begin{cases} a > 0, b > 0, c > 0, b > a\,, \\ (a+b)(b-a+c)\left(b^{1/2}-a^{1/2}\right) > 4ab\left(a^{1/2}+b^{1/2}\right)\,. \end{cases}
$$

Next, we will show the existence of the Hopf bifurcation of system (1) at equilibria O_i. Suppose $b = 4a$, then Eq. (2) can be rewritten as

$$
\lambda^3 + (3a+c)\lambda^2 + \tfrac{5}{3}ac\lambda + 16a^2c = 0\,. \tag{3}
$$

Assume $\lambda = \sigma i, \sigma > 0$ is a pure imaginary root of Eq. (3), then

$$
(\sigma i)^3 + (3a+c)(\sigma i)^2 + \tfrac{5}{3}ac(\sigma i) + 16a^2c = 0\,.
$$

It follows that

$$
\begin{cases} 3\sigma^2 - 5ac = 0\,, \\ (3a+c)\sigma^2 - 16a^2c = 0\,, \end{cases}
$$

then we have

$$\begin{cases} c_0 = \dfrac{33}{5}a\,, \\ \sigma_0 = \sqrt{11}a\,. \end{cases}$$

Since $a > 0$, then there exists a constant $\sigma > 0$ such that $\lambda = \sigma i$ is really a root of Eq. (3). Differentiating Eq. (3) with respect to c, one has

$$\frac{d\lambda}{dc} = -\frac{3\lambda^2 + 5a\lambda + 48a^2}{9\lambda^2 + (18a + 6c)\lambda + 5ac}\,,$$

then

$$\mathrm{Re}\left(\frac{d\lambda}{dc}\right)|_{c=c_0,\lambda=\sigma_0 i} = -\frac{275}{5158}a^2 < 0\,.$$

It is clear that the transversality condition is met. Therefore, system (1) bifurcation occurs at points O_1, O_2 with two limit cycles branching from the O_1, O_2 when parameter c decreases beyond the critical value $c = c_0$ according to the Kuznetso's Hopf bifurcation theory [23]. The stability and direction of the bifurcating periodic solutions can be determined by calculating the first Lyapunov coefficient. Let $a = 1, b = 4a = 4$, then the periodic solutions of system (1) with $c = c_0 = 33a/5 = 33/5$ are shown in Fig. 2. It is obvious that system (1) occurs independent of Hopf bifurcations at equilibria O_1, O_2.

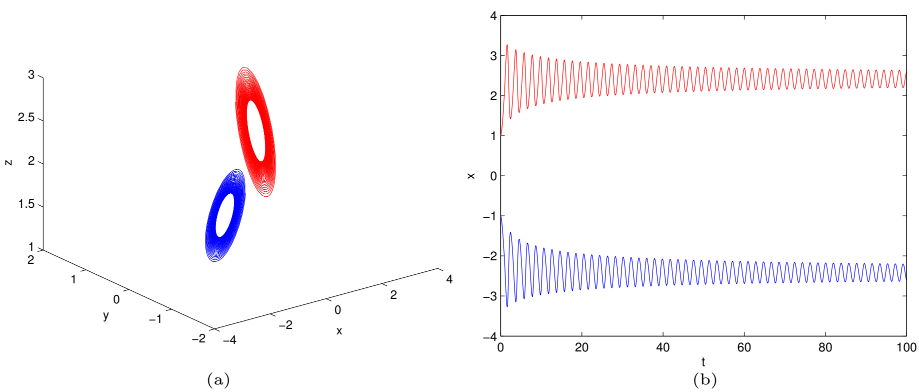

Fig. 2. (Color on-line) The limit cycles of system (1) with $c = 33/5$: (a) x–y–z; (b) time series.

4. Dynamic evolution and coexisting attractors

In this section, we will investigate the complex dynamical behaviors of system (1) intuitively. The evolution of the system status including stability, periodicity, chaos is presented by bifurcation diagrams, Lyapunov exponents, and phase portraits. The coexisting attractors *i.e.* multiple attractors with their own domains of attraction yield simultaneously with respect to different initial values are analyzed. The numerical calculations are presented by applying the fourth-order Runge–Kutta integrator with a fixed step size $\Delta t = 0.01$ and an absolute error bound of 10^5 at each step. The iteration time of the integrator is from $t = 0$ to $t = 300$. It is also verified numerically that the phase portraits and time series do not essentially change as the iteration time $t > 300$ (*e.g.* $t = 10^6$). The Lyapunov exponents are obtained by using the classic Wolf method [24]. All the simulation graphics are carried out by Matlab software platform.

4.1. For $b = 10$, $c = 4$ and varying a

Suppose $b = 10$, $c = 4$, then the bifurcation diagrams of the variable y *versus* $a \in [0, 8]$ from initial values $(1, 1, 1)$ (red) and $(-1, -1, 1)$ (blue) are obtained as shown in Fig. 3 (a). The Lyapunov exponents of system (1) *versus* $a \in [0, 8]$ from initial value $(1, 1, 1)$ are shown in Fig. 3 (b). It can be observed that system (1) performs stable, periodic, chaotic states as a changes. For some values of a, system (1) two attractors coexist with respect to initial values $(1, 1, 1)$, $(-1, -1, 1)$. It can be more clearly demonstrated by the phase diagram as follows.

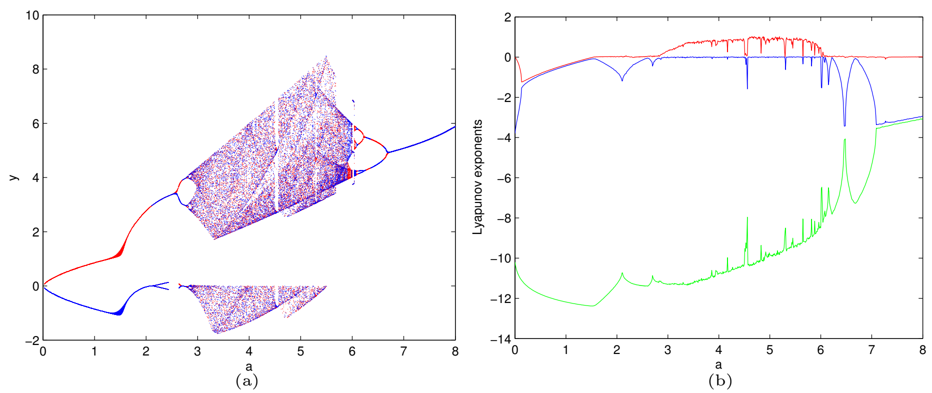

Fig. 3. (Color on-line) The bifurcation diagrams and Lyapunov exponents of system (1) with $b = 10$, $c = 4$ and $a \in [0, 8]$.

For $0 \leq a < 1.5595$, system (1) has coexisting point attractors. Let $a = 1$, then system (1) has stable equilibria $P_1(2.7021, 0.8545, 3.1623)$ and $P_2(-2.7021, -0.8545, 3.1623)$ with the same eigenvalues $\lambda_1 = -12.2014$, $\lambda_{2,3} = -0.3993 \pm 3.5991i$. The trajectories generated from initial values $(1, 1, 1)$ (red) and $(-1, -1, 1)$ (blue) eventually tend to the equilibria A_1, A_2 as shown in Fig. 4 (a). It means that in system (1) two stable point attractors coexist. For $a = 1.5595$, system (1) has equilibria $Q_1(2.8493, 1.1252, 3.9491)$ and $Q_2(-2.8493, -1.1252, 3.9491)$ with the same eigenvalues $\lambda_1 = -12.4405$, $\lambda_{2,3} = \pm 4.4785i$. It can be verified that system (1) shows double Hopf bifurcations at Q_1 and Q_2 with the generation of limit cycles. For $1.5595 \leq a \leq 2.1$, system (1) has coexisting periodic attractors. Let $a = 1.7$, the coexisting periodic attractors generate from initial values $(1, 1, 1)$ (red) and $(-1, -1, 1)$ (blue) are shown in Fig. 4 (b). For $2.2 \leq a \leq 2.6$, system (1) has only one 1-periodic attractor from some initial value as shown in Fig. 4 (c). For $a = 2.7, 2.8$, system (1) has one 2-periodic attractor as shown in Fig. 4 (d). For $2.9 \leq a \leq 5.9$, system (1) has one double-wing chaotic attractor as shown in Fig. 4 (e)–(f). For $a = 6$, system (1) two chaotic attractors coexist with respect to initial values $(1, 1, 1)$ (red) and $(-1, -1, 1)$ (blue) as shown in Fig. 4 (g). Their largest Lyapunov exponents are both LE $= 0.3637 > 0$. The chaotic attractors have similar structure and feature. For $a = 6.1, 6.2$, system (1) two 2-periodic attractors coexist with respect to initial values $(1, 1, 1)$ (red) and $(-1, -1, 1)$ (blue) as shown in Fig. 4 (h). For $6.3 \leq a \leq 6.5$, system (1) yields two 1-periodic attractors from initial values $(1, 1, 1)$ (red), $(-1, -1, 1)$ (blue) as shown in Fig. 4 (i). For $6.6 \leq a \leq 8$, system (1) has only one periodic attractor as shown in Fig. 4 (j).

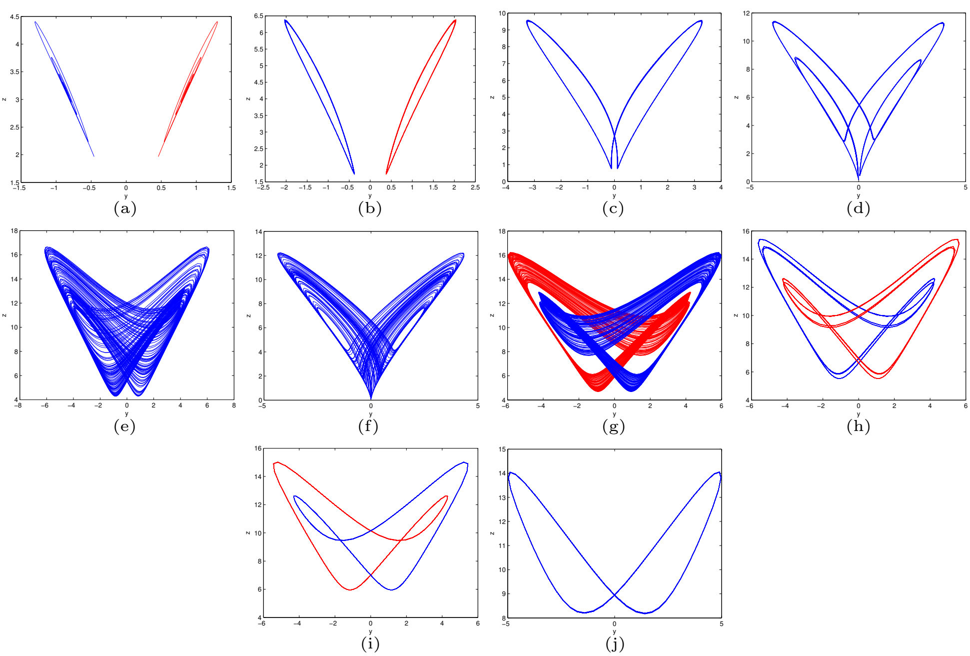

Fig. 4. (Color on-line) The phase plane of system (1): (a) $a=1$; (b) $a=1.7$; (c) $a=2.4$; (d) $a=2.8$; (e) $a=3$; (f) $a=5.9$; (g) $a=6$; (h) $a=6.2$; (i) $a=6.3$; (j) $a=6.8$.

4.2. For $a = 6$, $c = 4$ and varying b

Suppose $a = 6$, $c = 4$, then the bifurcation diagrams of the variable y *versus* $b \in [10, 25]$ from initial values $(1, 1, 1)$ (red) and $(-1, -1, 1)$ (blue) are shown in Fig. 5 (a). The Lyapunov exponents of system (1) *versus* $b \in [10, 25]$ from initial value $(1, 1, 1)$ is shown in Fig. 5 (b). It is clear that system (1) has only one chaotic attractor with $10 \leq b \leq 20.5$. When $20.6 \leq b \leq 21.2$, system (1) two chaotic attractors coexist according to the bifurcation diagram. Select $b = 20.8$, the coexisting chaotic attractors with respect to initial values $(1, 1, 1)$ (red) and $(-1, -1, 1)$ (blue) are shown in Fig. 6 (a). When $21.3 \leq b \leq 25$, system (1) has coexisting periodic attractors as shown in Fig. 6 (b).

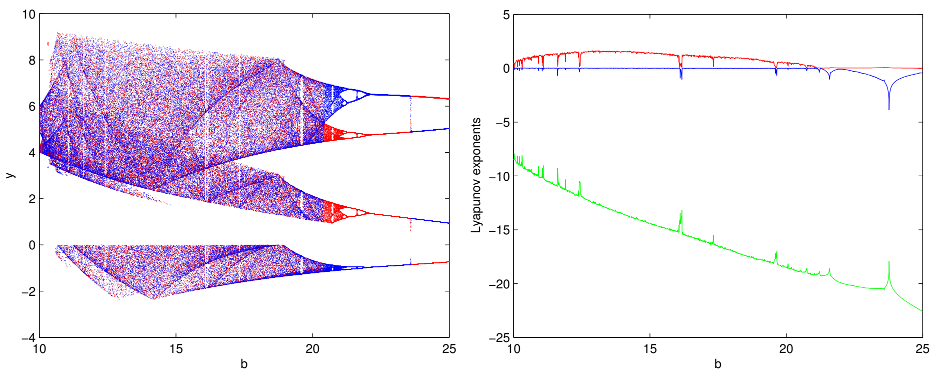

(a) (b)

Fig. 5. (Color on-line) The bifurcation diagrams and Lyapunov exponents of system (1) with $a = 6$, $c = 4$ and $b \in [10, 25]$.

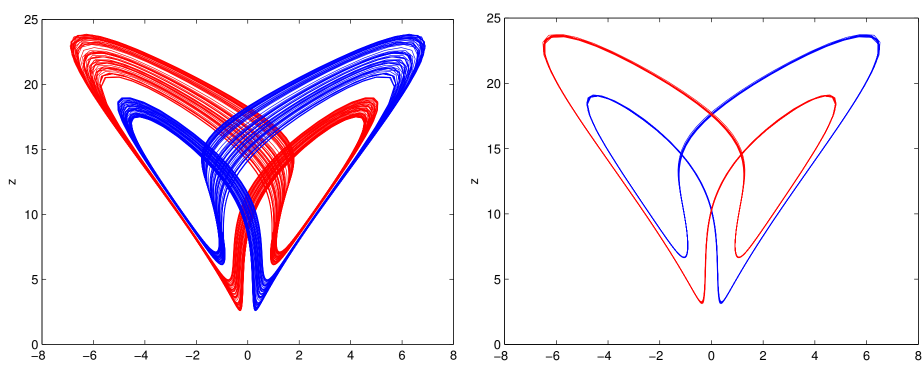

(a) (b)

Fig. 6. (Color on-line) The phase plane of system (1): (a) $b = 20.8$; (b) $a = 22.8$.

4.3. For $a = 6$, $b = 10$ and varying c

Suppose $a = 6$, $b = 10$, then the bifurcation diagrams of the variable y *versus* $c \in (0, 6)$ from initial values $(1, 1, 1)$ (red) and $(-1, -1, 1)$ (blue) are shown in Fig. 7 (a). The Lyapunov exponents of system (1) *versus* $c \in (0, 6)$

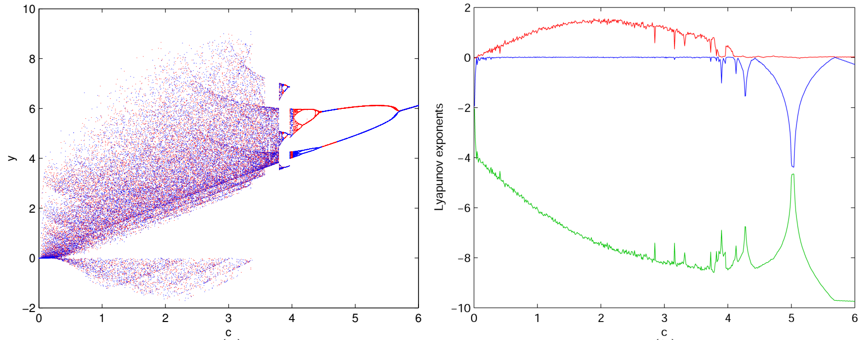

(a) (b)

Fig. 7. (Color on-line) The bifurcation diagrams and Lyapunov exponents of system (1) with $a = 6$, $b = 10$ and $c \in (0, 6)$.

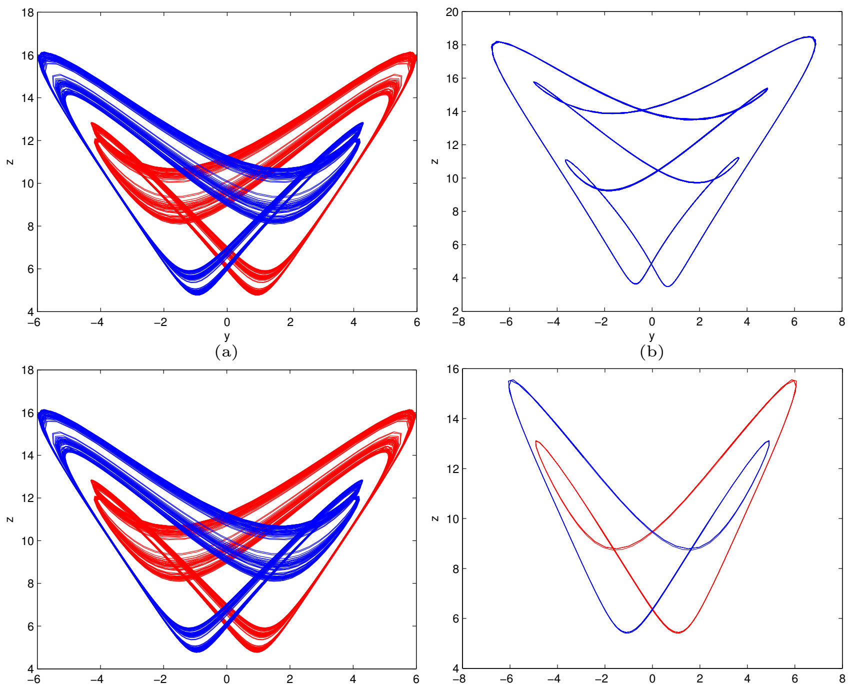

(a) (b) (c) (d)

Fig. 8. (Color on-line) The phase plane of system (1): (a) $c = 3.8$; (b) $c = 3.9$; (c) $c = 4.1$; (d) $c = 5$.

from initial value $(1,1,1)$ are shown in Fig. 7 (b). From the bifurcation diagram, we obtain that system (1) has a chaotic attractor with $0 < c \leq 3.8$. The chaotic attractor of system (1) with $c = 3.8$ is shown in Fig. 8 (a). When $c = 3.9$, system (1) has a periodic attractor as shown in Fig. 8 (b). When $c = 4,1$, system (1) has coexisting chaotic attractors corresponding to initial values $(1,1,1)$ (red) and $(-1,-1,1)$ (blue) as shown in Fig. 8 (c). When $4.2 \leq c \leq 5.7$, system (1) two periodic attractors coexist as shown in Fig. 8 (d). When $5.8 \leq c < 6$, system (1) has only one periodic attractor.

From the above analysis, we can easily conclude that system (1) performs chaotic motion in a wide range of parameters. The coexisting attractors including point, periodic, and chaotic attractors are prevalent in system (1). The dynamic behaviors of system (1) are not only dependent on the parameters, but also related to the initial conditions.

5. Conclusions

This paper presented a new 3D chaotic system with five quadratic nonlinearities. The basic behaviors of the system are analyzed. The dynamic evolution of the system is analyzed by bifurcation diagram, Lyapunov exponents and phase diagram. It is shown that the system generated chaotic attractors in a wide range of parameters. The coexisting attractors including point, periodic, and chaotic attractors of the system are investigated. Nowadays, the chaotic systems with coexisting attractors are of great theoretical and practical significance. More related studies of the coexisting attractors will be shown in our future paper.

REFERENCES

[1] E.N. Lorenz, *J. Atmos. Sci.* **20**, 130 (1963).
[2] O.E. Rössler, *Phys. Lett. A* **57**, 397 (1976).
[3] A.M. Rucklidge, *J. Fluid Mech.* **237**, 209 (1992).
[4] R. Genesio, A. Tesi, *Automatica* **28**, 531 (1992).
[5] J.C. Sprott, *Phys. Rev. E* **50**, 647 (1994).
[6] G. Chen, T. Ueta, *Int. J. Bifurc. Chaos* **9**, 1465 (1999).
[7] J. Lü, G. Chen, *Int. J. Bifurc. Chaos* **12**, 659 (2002).
[8] Y. Sun, G. Qi, Z. Wang, B.J. Wyk, *Acta Phys. Pol. B* **41**, 767 (2010).
[9] Z.C. Wei, *Phys. Lett. A* **376**, 102 (2011).
[10] S. Jafari, J.C. Sprott, S. Golpayegani, *Phys. Lett. A* **377**, 699 (2013).
[11] T. Gao, Z. Chen, Q. Gu, Z. Yuan, *Chaos Soliton Fract.* **35**, 390 (2008).
[12] Y. Li, X. Liu, G. Chen, X. Liao, *Int. J. Circ. Theory Appl.* **39**, 865 (2011).
[13] H. Bouraoui, K. Kemih, *Acta Phys. Pol. A* **123**, 259 (2013).

[14] R.B. Leipnik, T.A. Newton, *Phys. Lett. A* **86**, 63 (1981).

[15] W.B. Liu, G. Chen, *Int. J. Bifurc. Chaos* **14**, 1395 (2004).

[16] S. Dadras, H.R. Momeni, G. Qi, *Nonlinear Dyn.* **62**, 391 (2010).

[17] J.C. Sprott, X. Wang, G. Chen, *Int. J. Bifurc. Chaos* **23**, 1350093 (2013).

[18] C.B. Li, J.C. Sprott, *Int. J. Bifurc. Chaos* **23**, 1350199 (2013).

[19] S. Banerjee, *IEEE Trans. Circ. Syst.-I* **44**, 847 (1997).

[20] V.N. Chizhevsky, *J. Opt. B — Quantum Semiclass. Opt.* **2**, 711 (2000).

[21] S. Morfu, B. Nofiele, P. Marquie, *Phys. Lett. A* **367**, 192 (2007).

[22] Z. Hou *et al.*, *Int. J. Bifurc. Chaos* **20**, 557 (2010).

[23] Y.A. Kuznetsov, *Elements of Applied Bifurcation Theory*, Springer, New York 1998.

[24] A. Wolf, J.B. Swift, H.L. Swinney, J.A. Vastano, *Physica D* **16**, 285 (1985).